

Review

Polymer/Fullerene Nanocomposite for Optoelectronics—Moving toward Green Technology

Ayesha Kausar ^{1,2,3,*} , Ishaq Ahmad ^{1,2,3}, Malik Maaza ², M. H. Eisa ⁴ and Patrizia Bocchetta ^{5,*} 

¹ NPU-NCP Joint International Research Center on Advanced Nanomaterials and Defects Engineering, Northwestern Polytechnical University, Xi'an 710072, China

² UNESCO-UNISA Africa Chair in Nanosciences/Nanotechnology, iThemba LABS, Somerset West 7129, South Africa

³ NPU-NCP Joint International Research Center on Advanced Nanomaterials and Defects Engineering, National Centre for Physics, Islamabad 44000, Pakistan

⁴ Department of Physics, College of Science, Imam Mohammad Ibn Saud Islamic University (IMSIU), Riyadh 13318, Saudi Arabia

⁵ Department of Innovation Engineering, University of Salento, Edificio La Stecca, Via per Monteroni, 73100 Lecce, Italy

* Correspondence: dr.ayeshakauser@yahoo.com (A.K.); patrizia.bocchetta@unisalento.it (P.B.)

Abstract: Optoelectronic devices have been developed using the polymer/fullerene nanocomposite, as focused in this review. The polymer/fullerene nanocomposite shows significant structural, electronics, optical, and useful physical properties in optoelectronics. Non-conducting and conducting polymeric nanocomposites have been applied in optoelectronics, such as light-emitting diodes, solar cells, and sensors. Inclusion of fullerene has further broadened the methodological application of the polymer/fullerene nanocomposite. The polymeric matrices and fullerene may have covalent or physical interactions for charge or electron transportation and superior optical features. Green systems have also been explored in optoelectronic devices; however, due to limited efforts, further design innovations are desirable in green optoelectronics. Nevertheless, the advantages and challenges of the green polymer/fullerene nanocomposite in optoelectronic devices yet need to be explored.

Keywords: green; nanocomposite; fullerene; optoelectronic; solar cell; diode; sensor



Citation: Kausar, A.; Ahmad, I.; Maaza, M.; Eisa, M.H.; Bocchetta, P. Polymer/Fullerene Nanocomposite for Optoelectronics—Moving toward Green Technology. *J. Compos. Sci.* **2022**, *6*, 393. <https://doi.org/10.3390/jcs6120393>

Academic Editors: Francesco Tornabene and Thanasis Triantafyllou

Received: 18 October 2022

Accepted: 13 December 2022

Published: 16 December 2022

Publisher's Note: MDPI stays neutral with regard to jurisdictional claims in published maps and institutional affiliations.



Copyright: © 2022 by the authors. Licensee MDPI, Basel, Switzerland. This article is an open access article distributed under the terms and conditions of the Creative Commons Attribution (CC BY) license (<https://creativecommons.org/licenses/by/4.0/>).

1. Introduction

Optoelectronic devices have outstanding optical and electronic properties [1–3]. Optoelectronic devices can transform electrical energy into light energy using semiconducting materials [4,5]. Important optoelectronic devices include the light-emitting diode, the photovoltaic device, and the optical sensor [5–7]. The use of nanocomposites and green nanomaterials in optoelectronics has been investigated [8,9]. Nanocomposites with high optical transparency and electron transfer properties are preferred for optoelectronics devices. Nanocomposites have been used in the light-emitting diode and exhibit low price, high conductivity, and fine optical properties. In photovoltaic devices, nanocomposites provide high charge transfer, high hole transport, and enhanced power conversion efficiency [10]. Optical sensors have also been developed using nanocomposites for enhanced sensing properties and applications. Polymer/fullerene nanocomposites have been applied in optical devices [11], such as the light-emitting diode [12], the photovoltaic device [13], and the optical sensor [14]. Inclusion of the fullerene nanoparticle in polymers may form physical or covalent interactions with the polymeric matrices. The polymer/nanofiller may develop an interconnecting network to facilitate electron transference and photon transfer properties [15]. For green nanocomposite technology, polymer/fullerene nanocomposites have been developed and applied. However, extensive efforts are desirable for advanced green-fullerene-based optoelectronics.

In this review, the research progress on the fullerene- and polymer/fullerene-derived nanocomposite regarding optical devices is discussed. High-performance polymer/fullerene nanocomposites have been successfully used in the light-emitting diode, photovoltaics, and the optical sensor.

2. Optoelectronics

Polymer/nanocarbon nanocomposites have been applied in optical and electronic industries [16,17]. Accordingly, polymer/nanocarbon nanocomposites have been used in light-emitting diodes, sensors, and electronic devices [18–21]. Among nanocarbons, graphene, carbon nanotubes, nanodiamond, etc., have been found useful in next-generation devices [22–25]. Nanocomposites have been fabricated through in situ, solution, melt-processing, spin-coating, printing, and other chemical and physical methodologies [26–28]. Fullerene is an important type of hollow cage-like nanocarbon nanostructure. Fullerene is composed of sp^2 -hybridized carbon atoms with a π -conjugation system [29,30]. The fullerene molecule is constructed by polygons, i.e., five- to seven-membered rings in the structure. Fullerene with 60 carbon atoms is named the C_{60} fullerene molecule, also referred to as Buckminster fullerene. It was first discovered as a polygon with 60 vertices and 32 faces [31]. This object is like a football or a soccer ball. Hence, C_{60} is the most symmetrical form of fullerene, with superior optical, electrical, magnetic, and pharmaceutical properties, in addition to the properties of encapsulating small molecules for various industrial applications. The optical properties of fullerenes have been widely examined in different solvents through spectroscopic techniques. Furthermore, according to the laws of quantum mechanics, the nonlinear optical polarizability of fullerene molecules was calculated and found to be higher than that of the carbon nanotube [31]. An electrical property study of zero-dimensional fullerene showed that fullerenes have semiconducting-metallic transitions in the large electric field, similar to the one-dimensional carbon nanotube and two-dimensional graphene. The magnetic properties of fullerene have been studied using density functional theory. In the presence of a magnetic field, fullerene exhibits diamagnetism independent of a metallic or semiconducting nature, similar to the carbon nanotube. Among pharmaceutical properties, fullerenes have the ability to inhibit the access of toxins to the catalytic site of enzymes. Moreover, fullerenes may act as radical scavengers and antioxidants, like other nanocarbons. Similarly, C_{70} is a higher fullerene analogue having 70 carbon atoms. C_{70} has excellent catalytic and photovoltaic properties for relevant applications [32]. The important forms of fullerene include C_{60} and C_{70} molecules (Figure 1) [33]. The higher fullerene analogues have also been reported with large cage sizes and a higher number of carbon atoms [34]. Fullerenes have been prepared using numerous methods, such as arc discharge, laser irradiation, plasma technique, microwave synthesis, CO_2 reduction with metallic lithium, and chemical methods [35]. Among these techniques, the arc discharge method is a successful, advantageous, and widely used method to generate high-quality fullerene in high yield. The fullerene production time and method parameters are also easily controllable. The plasma technique and microwave synthesis also produce good-quality fullerene. However, the plasma and microwave techniques have lower yield, high cost, and complicated parameters involved, relative to the arc discharge method. The use of a chemical method usually yields byproducts and has lower fullerene quality compared to the other methods. Kroto et al. [36] synthesized fullerene via carbon source vaporization using the laser irradiation method. The resulting fullerene consisted of clusters of 60 carbon atoms. The plasma technique was used to form good-quality fullerenes [37]. Xie et al. [38] used the microwave plasma synthesis method to attain fullerenes from chloroform plasma in a low-pressure and high-temperature argon atmosphere. Chen and Lou [39] developed fullerene C_{60} by reduction of CO_2 using metallic lithium at 700 °C and 100 MPa. Scott et al. [40] adopted multi-step chemical conditions to convert the carbon precursor to fullerene C_{60} . Henceforth, several methods were used to synthesize fullerene structures, although all the techniques have relative advantages and disadvantages involved. Fullerene molecules have fine structural, electronic, optoelectronic, fluorescence, and photochemical

properties [41–44]. Substituted fullerene nanostructures have also been used to develop optoelectronics [45–47].

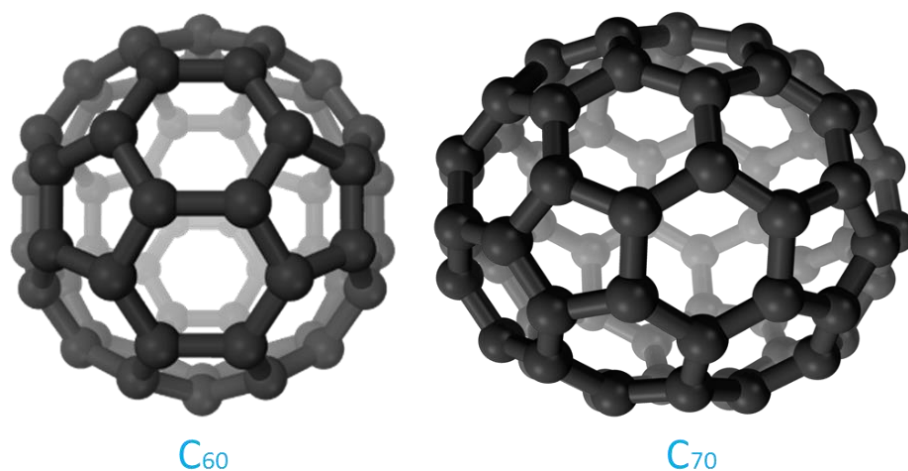


Figure 1. Comparison of C_{60} and C_{70} nanostructures.

Fullerene and derived fullerene molecules have been used in various technical areas, as shown in Figure 2 [48]. The applications of fullerene include solar cells, fuel cells, capacitors, sensors, catalysis, and adsorption. In optical devices, electron affinity, charge transference, optoelectronic features, band gap, and other tunable properties have been studied. The compatibility between the polymer and fullerene has been improved through using modified fullerene molecules and an appropriate polymer. Mostly, conjugated polymers have been found well matched with fullerenes. Especially, the π -conjugated structure of polythiophene has been found compatible with the fullerene sp^2 -hybridized nanocarbon structure [49]. Similarly, polythiophene derivatives have been found to be quite compatible with the fullerene molecule. Other conjugated polymers, such as polyaniline and polypyrrole, may also develop π - π stacking interactions with fullerene.

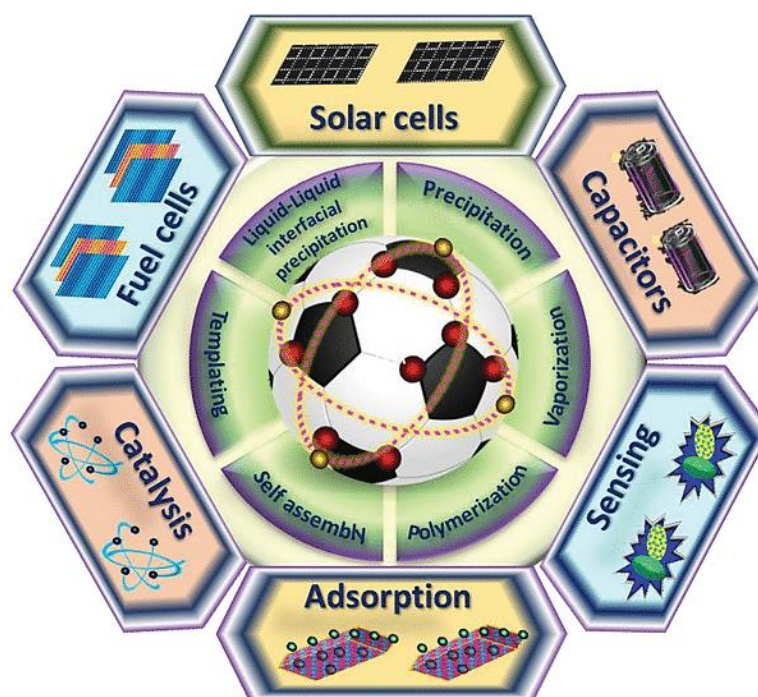


Figure 2. Synthesis, functionalization, and application of fullerene [48]. Reproduced with permission from Wiley.

3. Polymer/Fullerene Nanocomposite for LEDs: Insertion of Green Technology

The term “green technology” means the use of eco-friendly, renewable, and biodegradable materials for desired applications, i.e., optoelectronic devices [50]. In this regard, on the one hand, green polymers (naturally derived biodegradable) and green nanofillers have been used to construct these devices. On the other hand, green synthesis methodologies have been applied to develop desired biodegradable nanomaterials. The ecofriendly nanocomposites developed for optoelectronics have low cost, light weight, fine processability, and electrical and optical properties [51,52]. The green-nanomaterial-derived donor-acceptor structures possess fine photo-energy conversion for LED devices. Fullerene-based organic light-emitting diodes (OLEDs) have been focused on in the literature [53,54]. OLEDs with fullerene nanoparticles have been fabricated due to inexpensiveness and high efficiency for next-generation optoelectronics [55]. OLEDs have been designed using the polythiophene/fullerene nanocomposite (Figure 3) [56]. In this attempt, the promising solution-processing approach was used to form low-cost, flexible, and compact sensor arrays of polythiophene/fullerene. The novelty of the OLED sensing system relies on its workability in two operating modes, i.e., photoluminescence intensity and decay time detection modes. The dye-embedded polythiophene/fullerene-derived OLED had a fast photo-response toward red-emitting dye-based oxygen and glucose sensors. Another successful design for the LED is poly(3,4-ethylenedioxythiophene):polystyrene sulfonate (PEDOT:PSS) [57]. In another attempt [58], an OLED based on tetracene, indium tin oxide/poly(3,4-ethylenedioxythiophene):polystyrene sulfonate (ITO/PEDOT:PSS), polycyclopentadithiophene-benzothiadiazole (PCPDTBT), phenyl-C70-butyric acid methyl ester (PC₇₀BM), and phenyl-C71-butyric acid methyl ester (PC₇₁BM) has been reported. Figure 4 shows the chemical structures and energy-level diagrams of solar cell devices [58]. It has been observed that the HOMO-LUMO was 5.4 and 3.0 eV for tetracene. PCPDTBT revealed a HOMO-LUMO of 5.1 and 3.7 eV. Tetracene/PCPDTBT exhibited an energetic barrier of 0.3 eV for hole extraction. The results suggested that the presence of a conjugated system promotes electron transport and hole extraction processes. Kang et al. [59] proposed LED devices with a high power conversion efficiency of 3.1% (AM 1.5 irradiation) and luminance of 8000 cd/m² [60]. For green OLED technology, Herrera et al. [61] developed a nanocomposite system using a green design and fabrication route. Inclusion of a small amount of polymer/fullerene may modify the optical response of the LED or OLED. Nevertheless, more focused research efforts may be needed to develop green polymer/fullerene systems to be applied in diode-based devices. In this regard, novel solution-processable polymer/fullerene-based flexible conductors can be developed to replace the ITO/glass electrode in these devices. The main advantages of using polymer/fullerene-based materials in LEDs (relative to ITO or glass materials) include design flexibility, light weight, low cost, and high efficiency. In this regard, the development of new green polymer/fullerene systems and ecofriendly processing routes must be focused on to form next-generation efficient, green OLED devices.

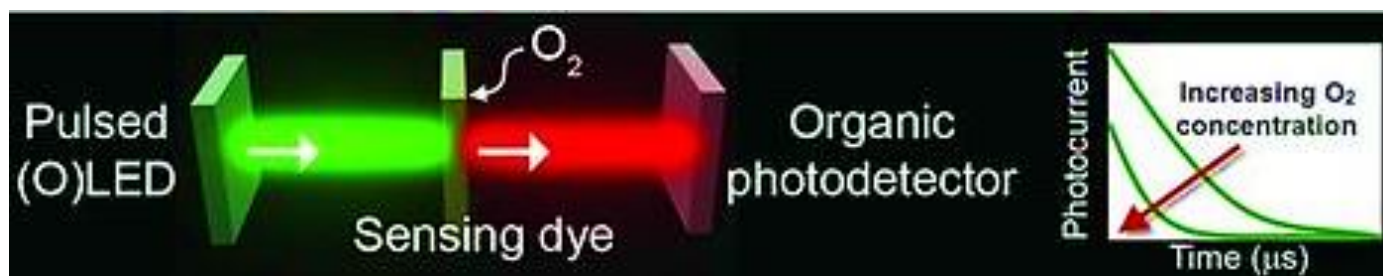


Figure 3. Organic light-emitting diode setup [56]. Reproduced with permission from Wiley.

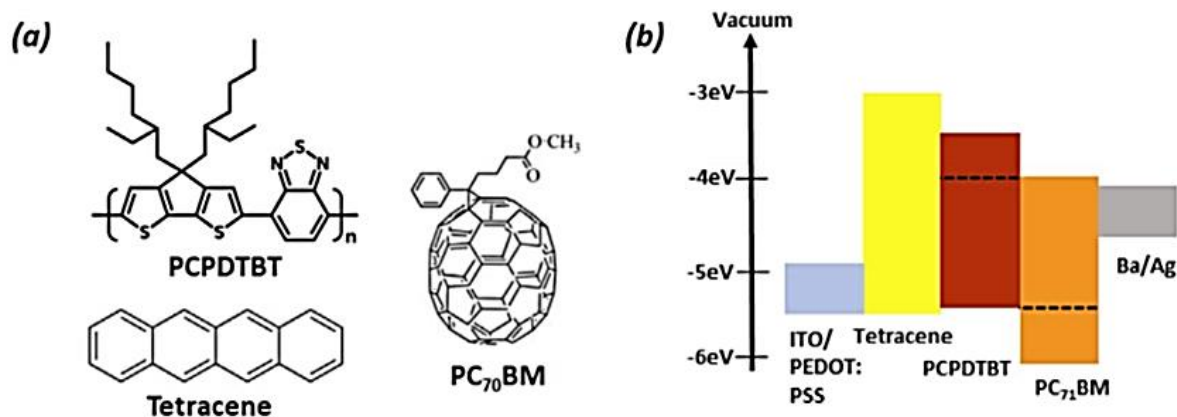


Figure 4. (a) Chemical structure of fullerene materials and (b) energy-level diagram of a bulk heterojunction device [58]. ITO/PEDOT:PSS = indium tin oxide/poly(3,4-ethylenedioxythiophene):polystyrene sulfonate; PCPDTBT = polycyclopentadithiophene-benzothiadiazole; PC₇₀BM = phenyl-C₇₀-butyric acid methyl ester; PC₇₁BM = phenyl-C₇₁-butyric acid methyl ester. Reproduced with permission from Wiley.

4. Polymer/Fullerene Nanocomposite in Solar Cells via the Green Approach

Advanced nanocomposites have always been of interest for application in solar cells [62–64]. Nanocomposites have good crystallinity, good contact between layers, good electrical conductivity, and promising light absorption properties, resulting in an improvement in the net efficiency of solar cells [65–67]. The design combination of a conducting polymer and nanocarbon nanofillers has resulted in enhanced solar cell efficiency [68]. Conjugated polymer/nanocarbon nanocomposites mostly act as electron donors, whereas the nanocarbon performs as the electron acceptor [69,70]. Generally, low-band-gap nanocomposites and blends have been found valuable in solar cell application [71]. Initially, various non-green polymeric nanocomposite systems were used in solar cell devices. PEDOT:PSS has been applied as an essential solar cell material [72]. PEDOT:PSS possesses fast electron and hole transportation features. The PEDOT:PSS-based nanocomposite was coated on the indium tin oxide (ITO) electrode using the spin-casting technique [73]. Consequently, the morphological, electron-conducting, and solar cell properties of PEDOT:PSS have been examined [74,75]. In this case, a solar cell efficiency of ~9% was obtained, which was high enough to obtain a high-performance solar cell device. Another successful system identified for the solar cell was poly(3-hexylthiophene-2,5-diyl):[6,6]-phenyl-C₆₁-butyric-acid-methyl-ester (P3HT:PCBM) [76]. For bulk heterojunction solar cell application, P3HT:PCBM film was developed through the spin-casting technique. The power conversion efficiency was found to be ~3.5%. For the P3HT:PCBM system [77], solvent methods, annealing, and drying approaches have been found useful. The microstructure analysis and optical micrographs have been obtained (Figure 5). Both micrometer-size crystalline domains and small domains (<200 nm) have been detected in the micrographs of P3HT:PCBM films [77]. It has been observed that the presence of impurities may produce inhomogeneities in the samples. The spin-coated and slow-dried nanocomposite showed homogeneous dispersion; however, impurities were still present in the sample. An important solar cell system was reported by Roy et al. [78]. Poly(methyl methacrylate) (PMMA), fullerene, quantum dots, single-walled carbon nanotubes, and reduced graphene oxide were used (Figure 6). Here, fullerene addition affected the charge carrier ability of the nanocomposites. With fullerene addition, the power conversion efficiency improved up to 1.15% (Table 1) [78]. PMMA and fullerene and other nanocarbons have the ability to develop interconnecting pathways for electron conduction [79,80]. Later research shifted toward the use of green designed materials and green synthesis approaches in solar cells.

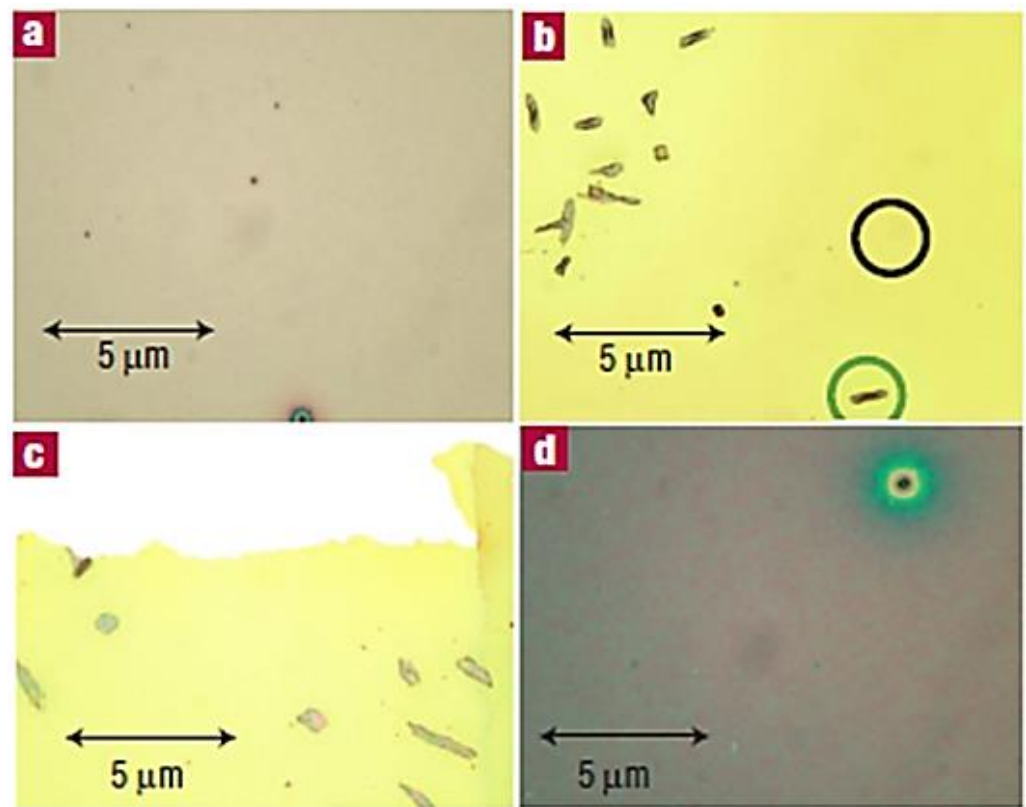


Figure 5. Optical microscope images for P3HT:PCBM film: (a) untreated (i.e., fast spin coated), (b) thermally annealed, (c) vapor annealed, and (d) slow dried. Inhomogeneities produced by impurities in (d) (upper-right corner of image) can often be seen in spin-coated P3HT:PCBM films [77]. P3HT:PCBM = poly(3-hexylthiophene):[6,6]-phenyl C₆₁-butyric acid methyl ester. Reproduced with permission from Nature.

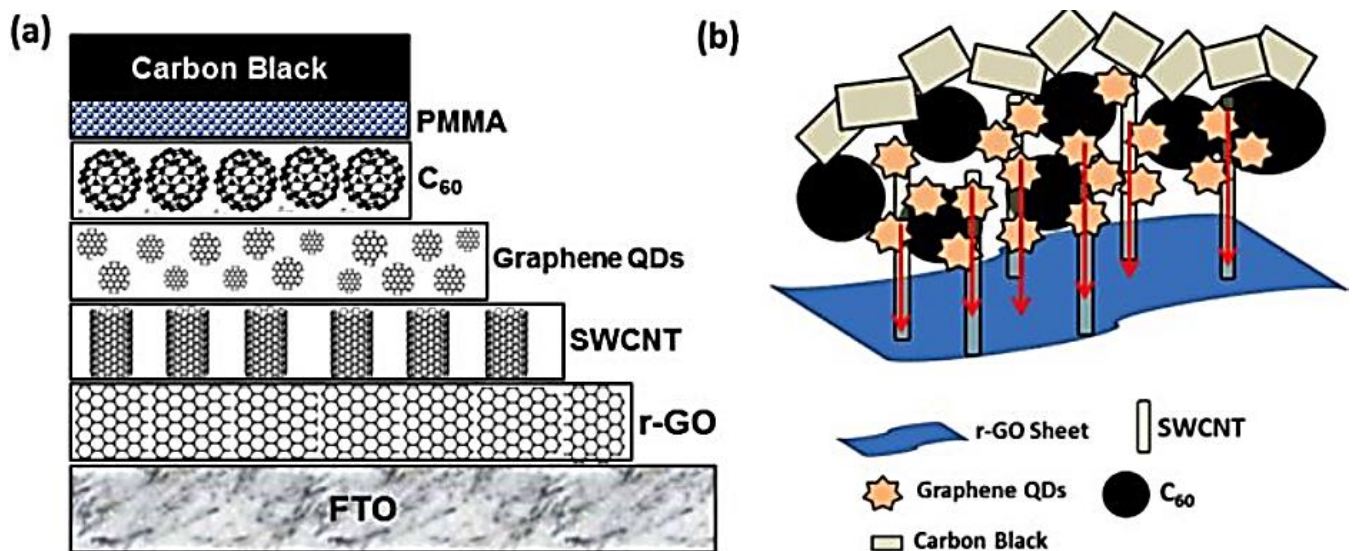


Figure 6. Schematic diagram of (a) sequential fabrication of solar cells using different allotropes of carbon and (b) probable arrangement of different allotropes used during sequential fabrication of carbon solar cells [78]. PMMA = poly(methyl methacrylate); QD = quantum dot; SWCNT = single-walled carbon nanotube; r-GO = reduced graphene oxide. Reproduced with permission from ACS.

Table 1. Solar cell parameters of nanocarbon-based solar cells [78]. PMMA/C₆₀ = poly(methyl methacrylate)/fullerene C₆₀; PCE = photo-conversion efficiency; J_{sc} = short-circuit current density; Voc = open-circuit voltage; FF = fill factor. Reproduced with permission from ACS.

Cell	Voc (mV)	Jsc (mA·cm ⁻²)	FF	PCE (%)
No PMMA/C ₆₀	500	1.54	0.56	0.56
PMMA/C ₆₀	506	3.93	0.59	1.15

For green nanocomposite technology, polymer/fullerene systems have been designed and studied in the literature [81]. However, limited reports have focused on the use of green polymers and green fabrication routes for solar cells. Amb et al. [82] designed conjugated polymer/fullerene-based blue-green solar cells using the thin-film deposition technique, i.e., spin coating. They reported a blue-green-colored low-bandgap polymer (PGREEN)-based nanocomposite (Figure 7) [82]. The poly(3-hexylthiophene):(6,6)-phenyl-C61-butyric acid methyl ester (PCBM)-based nanocomposite was used as a light-absorbing layer. The spin-coated PCBM-based PGREEN revealed fine solar cell performance. The donor-acceptor bulk heterojunction solar cell design is given in Figure 8 [82]. The J-V features of the devices with the PGREEN nanocomposite are also give in Figure 8. With fullerene inclusion, the solar cell system had a power conversion efficiency of up to 1.92%. The results were observed due to the high electron mobility of fullerenes effectively promoting charge dissociation and transportation in solar cell devices. Khlyabich et al. [83] reviewed the use of polymer/fullerene designs using non-halogenated solvent systems, such as toluene and tetrahydrofuran. Recent efforts have focused on the replacement of non-halogenated organic solvents with green solvent systems, such as water and ionic liquid [84]. The green-solvent-based methods have been successful in the fabrication of photoactive fullerene solar cells. Lee et al. [85] also proposed routes to develop polymer solar cells with a power conversion efficiency of >17%. Such solar cells have been developed using the green solvent and green fabrication route (Figure 9) [85]. The appropriate material design, choice of processing technique, and choice of solvent may lead to the formation of green solar cells on a large scale. Thus, green polymer/fullerene systems provide a roadmap to design efficient green future solar cell materials. The latest advances in perovskite solar cells have also pointed out the use of fullerene molecules [86]. Thus, fullerene-based high-efficiency perovskite solar cells have been reported. The inclusion of fullerene molecules in interfacial selective electron extraction layers in perovskite have remarkably improved the solar cell efficiency and device stability [87]. In this regard, facile processing methods have been used to form perovskite films. In conclusion, fullerene-based perovskite solar cells have been produced for large-scale and commercial applications [88].



Figure 7. A green polymer/fullerene solar cell [82]. Reproduced with permission from ACS.

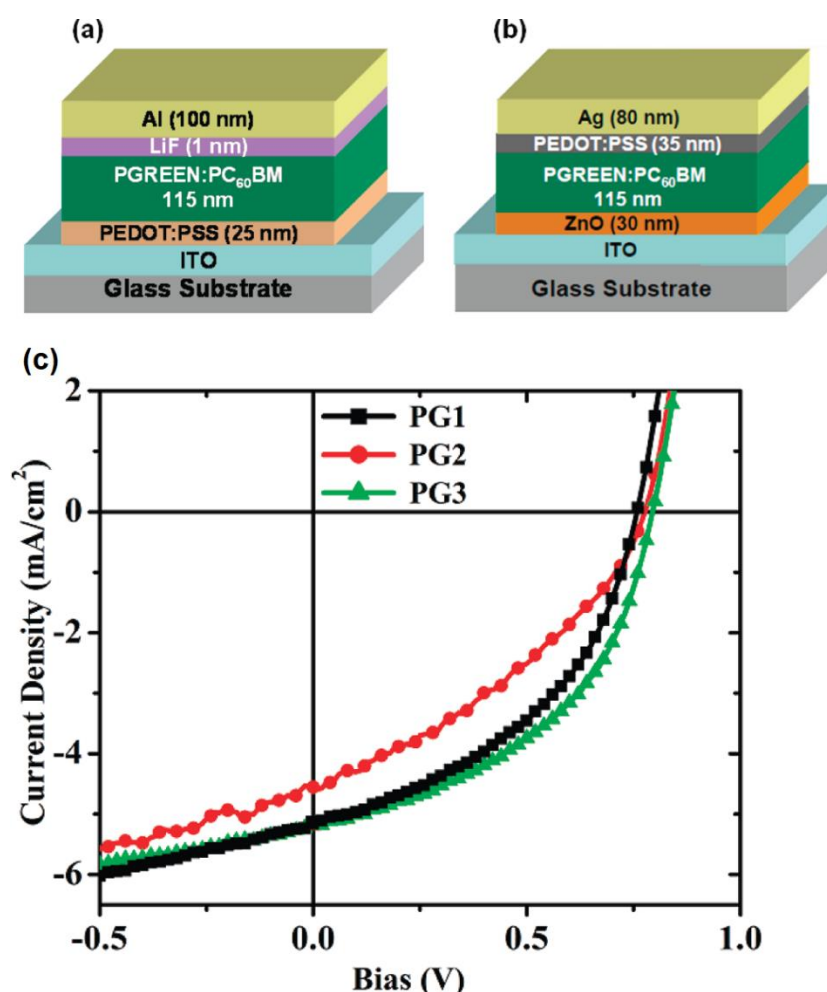


Figure 8. Schematic diagram of PGREEN polymer solar cells with (a) conventional and (b) inverted geometry. (c) Current–voltage plots for illuminated conventional geometry cells (0.04 cm^2) for each of the three polymer batches produced under identical processing conditions. [82]. Reproduced with permission from ACS.

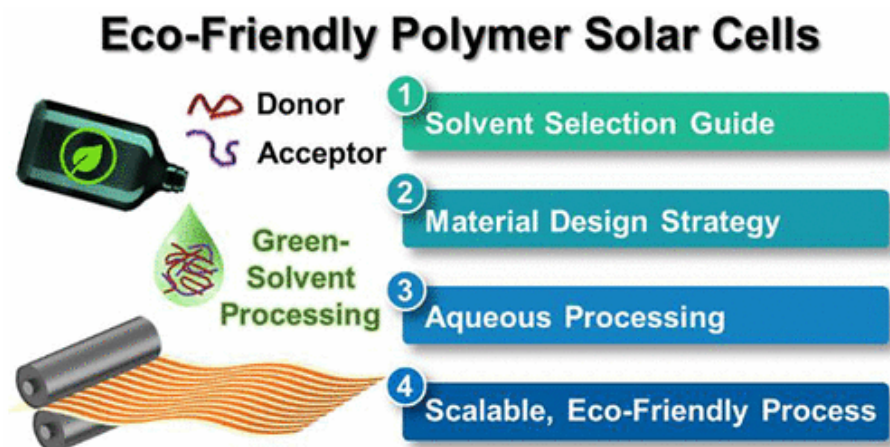


Figure 9. Design of eco-friendly polymer solar cells [85]. Reproduced with permission from ACS.

5. Polymer/Fullerene for Optical Sensors: On the Road to Green Nanocomposites

Optical or electronic sensors have been reported using various relevant materials [89–91]. Conducting polymers have notable electron donor or acceptor proper-

ties valuable for sensor applications [92]. Consequently, conducting polymers have been used for optical, electrical, and sensing properties. The conducting polymer/nanocarbon nanocomposite has also been prepared and analyzed [93,94]. Nanocarbon nanostructures, such as graphene and carbon nanotubes, have been applied in sensing applications [95]. Among conducting polymers, polyaniline has been frequently chosen for optical sensing [96–98]. The sensing mechanism of the nanocomposite has been found dependent on the matrix–nanofiller interactions and interface development [99–101]. Similarly, the conducting polymer/fullerene nanocomposite has been fabricated using appropriate techniques [102–104]. In this regard, organic thin-film photodiode (OPD) devices have been developed for optical sensors [105]. Optical sensors have been formed through advanced techniques, such as printing, spraying, and spin casting [106]. Analytes have been detected using the fluorescence/luminescence detection technique with the OPD device [107]. Various conducting polymers, such as P3HT, PCBM, PEDOT:PSS, and PEDOT:PSS, have been applied in optical sensors. In optical sensors, fullerene molecules, such as C₆₀ and C₇₀, have been applied [108–110]. Amao et al. [111] fabricated an optical temperature sensor using a PMMA- and C₆₀-derived nanocomposite. The fluorescence intensity was explored in the range of 260–373 K. However, initial efforts on optical sensors have focused on the use of non-green materials and methods. Similar to solar cells, the technology for optical sensors has also been upgraded toward the use of green nanocomposite or green synthesis routes. For green nanocomposite technology, Rather et al. [112] developed a green polymer/fullerene optical sensor. The sensor was used for sensing bisphenol A in the concentration range of 74 nM to 0.23 M. A detection limit of 3.7 nM was observed. Zhang et al. [113] formed a porphyrin–diazocine–porphyrin–fullerene (PDP–C₆₀)- and porphyrin–diazocine–porphyrin–fullerene/glassy carbon electrode (PDP–C₆₀/GCE)-based optical sensor. The fine dopamine detection of the PDP–C₆₀/GCE nanocomposite electrode was analyzed. Figure 10 shows the cyclic voltammetry (CV) curves of the PDP–C₆₀/GCE nanocomposite [113]. The linear relationship between the peak currents and scan rates of the nanocomposite revealed fine sensing performance toward dopamine. The sensor shows a detection limit of 0.015 μM. Here again, the development and analysis of better polymer/fullerene-based green nanocomposite systems have been found essential to obtain high-performance advanced optical sensors.

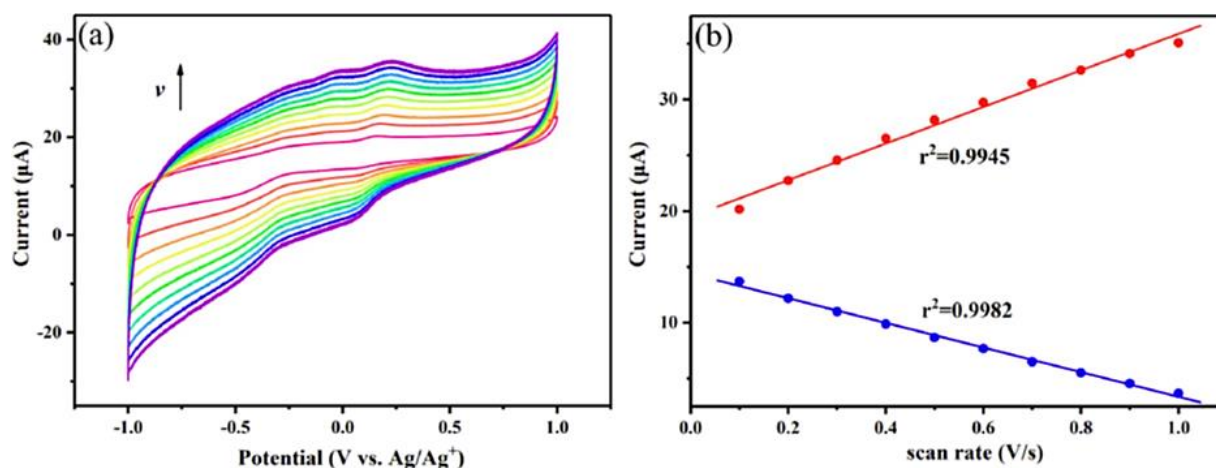


Figure 10. (a) CV curves of PDP–C₆₀/GCE nanocomposite (pH 7.4) containing 400 μM of DA at different scan rates (v) ranging from 0.1 to 1.0 V s^{−1} and (b) linear relationship between the peak currents and scan rates [113]. CV = cyclic voltammetry; PDP–C₆₀/GCE = porphyrin–diazocine–porphyrin–fullerene/glassy carbon electrode; DA = dopamine. Reproduced with permission from Elsevier.

6. Future and Conclusions

Polymer/fullerene nanocomposites have fine optical, electronic, electrical, thermal, mechanical, sensing, and other valuable properties for technical applications. Fullerene and fullerene-derived nanomaterials have led to high-performance optoelectronics, such as the light-emitting diodes, photovoltaic devices, and optical sensors (Table 2).

Table 2. Stipulations of the polymer/fullerene nanocomposite in optoelectronic applications.

Polymer	Nanofiller	Property/Application	Ref.
Polythiophene	Fullerene	OLED device, photoluminescence, oxygen sensitivity	[56]
Poly(3,4-ethylenedioxythiophene):polystyrene sulfonate	Fullerene	OLED device, energetic barrier, hole extraction	[57]
Polycyclopenta-dithiophene-benzothiadiazole	Fullerene	OLED device, energetic barrier, hole extraction	[58]
Poly(3,4-ethylenedioxythiophene):polystyrene sulfonate	Fullerene	LED, power conversion efficiency 3.1% (AM 1.5 irradiation), luminance of 8000 cd/m ²	[59]
Poly(3-hexylthiophene-2,5-diyl):[6,6]-phenyl-C ₆₁ -butyric-acid-methyl-ester	Fullerene	Bulk heterojunction solar cell, power conversion efficiency, solar cell efficiency ~3.5%, electron transport, interface formation	[76]
Poly(3-hexylthiophene):[6,6]-phenyl C ₆₁ -butyric acid methyl ester	Fullerene	Optical micrographs, PCBM domains <200	[77]
Poly(methyl methacrylate)	Fullerene	Photovoltaic device, power conversion efficiency 1.15%, short-circuit current density 3.93 mA/cm ² , open-circuit voltage 506 mV, fill factor 0.59	[78]
Poly(3-hexylthiophene):(6,6)-phenyl-C ₆₁ -butyric acid methyl ester	Fullerene	Power conversion efficiency 1.92%	[82]
Polymer	Fullerene	Power conversion efficiency >17%	[85]
Poly(methyl methacrylate)	Fullerene	Optical sensor, fluorescence intensity 260–373 K	[111]
Polymer	Fullerene	Bisphenol A detection limit 3.7 nM	[112]
Porphyrin–diazocine–porphyrin	Fullerene	Optical sensor, dopamine, detection limit 0.015 μM	[113]

In such devices, mostly conducting polymers, such as polyaniline, polypyrrole, polythiophene, and poly(3,4-ethylenedioxythiophene), have been used [114–116]. To further enhance properties, nanocarbon nanoparticles are incorporated in conjugated polymers. The optoelectronic performance of polymer/fullerene nanomaterials is dependent on the fullerene dispersion and matrix–fullerene interactions. However, non-conjugated polymers have also been applied in optoelectronics devices. The future of polymer/fullerene nanocomposite-derived optoelectronics depends on the design novelties and fullerene dispersion and functionality in the conjugated polymers. For all types of optoelectronic devices, facile fabrication techniques, modified polymers, and functional fullerene nanoparticles

need to be incorporated. The systems developed for green polymer/fullerene nanocomposite technology show fine performance; however, further efforts must be made to develop green LEDs, OLEDs, solar cells, and optical sensors. Thus, in recent years, great advancements have been made in fabrication skills and integration of optoelectronic nanomaterials to improve performance and the final device architecture. For next-generation optoelectronics, fullerene-based green nanocomposites can be studied as promising candidates for creating miscellaneous flexible and miniature devices. The recent advances in optoelectronics, in material selection and fabrication approaches, have proposed the use of thiophene-derived green polymers and green synthesized/functionalized fullerenes. These materials are considered ideal to obtain eco-friendly energy conversion, sensing, and diode devices. In this regard, green nanocomposites processed through the eco-friendly solution route can lead to the best results. However, the challenges and future research direction in this area need to be analyzed.

In short, this review summarizes the critical properties and performance of the polymer/fullerene nanocomposite in optoelectronic devices. Numerous facile fabrication and design approaches have been used to fabricate these technical devices. The versatility of the polymer/fullerene nanocomposite for optoelectronic devices relies on processing, fullerene dispersal, matrix–nanofiller compatibility, and essential properties. Future advancements in the field of the polymer/fullerene nanocomposite may develop advanced next-generation green optoelectronic devices.

Author Contributions: Conceptualization, A.K.; data curation, A.K.; writing of original draft preparation, A.K.; Review and editing, A.K.; I.A.; M.M.; M.H.E.; P.B. All authors have read and agreed to the published version of the manuscript.

Funding: This research received no external funding.

Conflicts of Interest: The authors declare no conflict of interest.

References

1. Kausar, A. Green nanocomposites for energy storage. *J. Compos. Sci.* **2021**, *5*, 202. [[CrossRef](#)]
2. Marchante Rodriguez, V.; Grasso, M.; Zhao, Y.; Liu, H.; Deng, K.; Roberts, A.; Appleby-Thomas, G.J. Surface damage in woven carbon composite panels under orthogonal and inclined high-velocity impacts. *J. Compos. Sci.* **2022**, *6*, 282. [[CrossRef](#)]
3. Kausar, A. Progress in green nanocomposites for high-performance applications. *Mater. Res. Innov.* **2021**, *25*, 53–65. [[CrossRef](#)]
4. Kausar, A. Carbon nanopeapod encapsulating fullerene and inorganic nanoparticle toward polymeric nanocomposite: Tailored features and promises. *Polym. Plast. Technol. Mater.* **2022**, *61*, 1481–1502.
5. Kausar, A. Polymer/carbon-based quantum dot nanocomposite: Forthcoming materials for technical application. *J. Macromol. Sci. Part A* **2019**, *56*, 341–356. [[CrossRef](#)]
6. Kamanina, N.; Toikka, A.; Kvashnin, D. Nanostructuring Impact on the Basic Properties of the Materials: Novel Composite Carbon Nanotubes on a Copper Surface. *J. Compos. Sci.* **2022**, *6*, 181. [[CrossRef](#)]
7. Kausar, A. A review of high performance polymer nanocomposites for packaging applications in electronics and food industries. *J. Plast. Film Sheeting* **2020**, *36*, 94–112. [[CrossRef](#)]
8. Kausar, A. Polymer/Nanocarbon Nanocomposite-Based Eco-friendly Textiles. In *Handbook of Nanomaterials and Nanocomposites for Energy and Environmental Applications*; Springer: Berlin/Heidelberg, Germany, 2021; pp. 2917–2939.
9. Kausar, A. Conjugated Polymer/Graphene Oxide Nanocomposites—State-of-the-Art. *J. Compos. Sci.* **2021**, *5*, 292. [[CrossRef](#)]
10. Kausar, A.; Bocchetta, P. Polymer/Graphene Nanocomposite Membranes: Status and Emerging Prospects. *J. Compos. Sci.* **2022**, *6*, 76. [[CrossRef](#)]
11. Zheng, B.; Yue, Y.; Ni, J.; Sun, R.; Min, J.; Wang, J.; Jiang, L.; Huo, L. An end-capped strategy for crystalline polymer donor to improve the photovoltaic performance of non-fullerene solar cells. *Sci. China Chem.* **2022**, *65*, 964–972. [[CrossRef](#)]
12. Ilmi, R.; Al-Sharji, H.; Khan, M.S. Recent Progress in Indacenodithiophene-Based Acceptor Materials for Non-Fullerene Organic Solar Cells. *Top. Curr. Chem.* **2022**, *380*, 18. [[CrossRef](#)] [[PubMed](#)]
13. Vuk, D.; Radovanović-Perić, F.; Mandić, V.; Lovrinčević, V.; Rath, T.; Panžić, I.; Le-Cunff, J. Synthesis and Nanoarchitectonics of Novel Squaraine Derivatives for Organic Photovoltaic Devices. *Nanomaterials* **2022**, *12*, 1206. [[CrossRef](#)] [[PubMed](#)]
14. Gonzalez Lopez, E.J.; Sarotti, A.M.; Martínez, S.R.; Macor, L.P.; Durantini, J.E.; Renfige, M.; Gervaldo, M.A.; Otero, L.A.; Durantini, A.M.; Durantini, E.N. BOPHY-Fullerene C₆₀ Dyad as a Photosensitizer for Antimicrobial Photodynamic Therapy. *Chem. A Eur. J.* **2022**, *28*, e202103884.
15. Šupová, M.; Martynková, G.S.; Barabaszová, K. Effect of nanofillers dispersion in polymer matrices: A review. *Sci. Adv. Mater.* **2011**, *3*, 1–25. [[CrossRef](#)]

16. Jouni, M.; Djurado, D.; Massardier, V.; Boiteux, G. A representative and comprehensive review of the electrical and thermal properties of polymer composites with carbon nanotube and other nanoparticle fillers. *Polym. Int.* **2017**, *66*, 1237–1251. [[CrossRef](#)]
17. Forrest, S.R.; Thompson, M.E. Introduction: Organic electronics and optoelectronics. *Chem. Rev.* **2007**, *107*, 923–925. [[CrossRef](#)]
18. Sun, Y.; Zeng, W.; Sun, H.; Luo, S.; Chen, D.; Chan, V.; Liao, K. Inorganic/polymer-graphene hybrid gel as versatile electrochemical platform for electrochemical capacitor and biosensor. *Carbon* **2018**, *132*, 589–597. [[CrossRef](#)]
19. Bhadra, S.; Rahaman, M.; Khanam, P.N. Electrical and Electronic Application of Polymer–Carbon Composites. In *Carbon-Containing Polymer Composites*; Springer: Berlin/Heidelberg, Germany, 2019; pp. 397–455.
20. Yogeswaran, N. *Graphene Field Effect Transistor Based Pressure Sensors for Tactile Sensing Applications*; University of Glasgow: Glasgow, UK, 2019.
21. Kholmanov, I.N.; Magnuson, C.W.; Piner, R.; Kim, J.Y.; Aliev, A.E.; Tan, C.; Kim, T.Y.; Zakhidov, A.A.; Sberveglieri, G.; Baughman, R.H. Optical, electrical, and electromechanical properties of hybrid graphene/carbon nanotube films. *Adv. Mater.* **2015**, *27*, 3053–3059. [[CrossRef](#)]
22. Das, D.; Rahaman, H. *Carbon Nanotube and Graphene Nanoribbon Interconnects*; CRC Press: Boca Raton, FL, USA, 2017.
23. Biswas, C.; Lee, Y.H. Graphene versus carbon nanotubes in electronic devices. *Adv. Funct. Mater.* **2011**, *21*, 3806–3826. [[CrossRef](#)]
24. Yamashita, S. A tutorial on nonlinear photonic applications of carbon nanotube and graphene. *J. Light. Technol.* **2011**, *30*, 427–447. [[CrossRef](#)]
25. Song, N.; Jiao, D.; Cui, S.; Hou, X.; Ding, P.; Shi, L. Highly anisotropic thermal conductivity of layer-by-layer assembled nanofibrillated cellulose/graphene nanosheets hybrid films for thermal management. *ACS Appl. Mater. Interfaces* **2017**, *9*, 2924–2932. [[CrossRef](#)] [[PubMed](#)]
26. Boysen, R.I.; Schwarz, L.J.; Nicolau, D.V.; Hearn, M.T. Molecularly imprinted polymer membranes and thin films for the separation and sensing of biomacromolecules. *J. Sep. Sci.* **2017**, *40*, 314–335. [[CrossRef](#)] [[PubMed](#)]
27. Müller, C.; Aghamohammadi, M.; Himmelberger, S.; Sonar, P.; Garriga, M.; Salleo, A.; Campoy-Quiles, M. One-step macroscopic alignment of conjugated polymer systems by epitaxial crystallization during spin-coating. *Adv. Funct. Mater.* **2013**, *23*, 2368–2377. [[CrossRef](#)]
28. Abdelghani, R.; Hassan, H.S.; Morsi, I.; Kashyout, A. Nano-architecture of highly sensitive SnO₂-based gas sensors for acetone and ammonia using molecular imprinting technique. *Sens. Actuators B Chem.* **2019**, *297*, 126668. [[CrossRef](#)]
29. Radford, C.L.; Mudiyansele, P.D.; Stevens, A.L.; Kelly, T.L. Heteroatoms as Rotational Blocking Groups for Non-Fullerene Acceptors in Indoor Organic Solar Cells. *ACS Energy Lett.* **2022**, *7*, 1635–1641. [[CrossRef](#)]
30. Tian, C.; Sun, C.; Chen, J.; Song, P.; Hou, E.; Xu, P.; Liang, Y.; Yang, P.; Luo, J.; Xie, L. Fullerene derivative with flexible alkyl chain for efficient tin-based perovskite solar cells. *Nanomaterials* **2022**, *12*, 532. [[CrossRef](#)]
31. Krätschmer, W.; Lamb, L.D.; Fostiropoulos, K.H.D.R.; Huffman, D.R. Solid C₆₀: A new form of carbon. *Nature* **1990**, *347*, 354–358.
32. Sachdeva, S.; Singh, D.; Tripathi, S. Optical and electrical properties of fullerene C₇₀ for solar cell applications. *Opt. Mater.* **2020**, *101*, 109717. [[CrossRef](#)]
33. Blanter, M.S.; Borisova, P.A.; Brazhkin, V.V.; Lyapin, S.G.; Sviridova, T.A.; Filonenko, V.P.; Kondratev, O.A. The influence of metals on the phase transformations of fullerenes at high pressure and high temperatures. *Mater. Lett.* **2022**, *318*, 132199. [[CrossRef](#)]
34. Wang, W.; Hanindita, F.; Hamamoto, Y.; Li, Y.; Ito, S. Fully conjugated azacorannulene dimer as large diaza[80]fullerene fragment. *Nat. Commun.* **2022**, *13*, 1498. [[CrossRef](#)]
35. Mojica, M.; Alonso, J.A.; Méndez, F. Synthesis of fullerenes. *J. Phys. Org. Chem.* **2013**, *26*, 526–539. [[CrossRef](#)]
36. Kroto, H.W.; Heath, J.R.; O'Brien, S.C.; Curl, R.F.; Smalley, R.E. C₆₀: Buckminsterfullerene. *Nature* **1985**, *318*, 162–163. [[CrossRef](#)]
37. Timerkaev, B.; Gevorgyan, R.; Zalyalieva, A.; Timerkaeva, D. Plasma-Chemical Synthesis of Nanodiamonds on the Surface of a Microarc Discharge Cathode. *J. Eng. Phys. Thermophys.* **2022**, *95*, 1201–1206. [[CrossRef](#)]
38. Xie, S.-Y.; Huang, R.-B.; Yu, L.-J.; Ding, J.; Zheng, L.-S. Microwave synthesis of fullerenes from chloroform. *Appl. Phys. Lett.* **1999**, *75*, 2764–2766. [[CrossRef](#)]
39. Chen, C.; Lou, Z. Formation of C₆₀ by reduction of CO₂. *J. Supercrit. Fluids* **2009**, *50*, 42–45. [[CrossRef](#)]
40. Scott, L.T. Methods for the chemical synthesis of fullerenes. *Angew. Chem. Int. Ed.* **2004**, *43*, 4994–5007. [[CrossRef](#)]
41. Shen, Y.; Nakanishi, T. Fullerene assemblies toward photo-energy conversions. *Phys. Chem. Chem. Phys.* **2014**, *16*, 7199–7204. [[CrossRef](#)]
42. Babu, S.S.; Möhwald, H.; Nakanishi, T. Recent progress in morphology control of supramolecular fullerene assemblies and its applications. *Chem. Soc. Rev.* **2010**, *39*, 4021–4035. [[CrossRef](#)]
43. Jariwala, D.; Sangwan, V.K.; Lauhon, L.J.; Marks, T.J.; Hersam, M.C. Carbon nanomaterials for electronics, optoelectronics, photovoltaics, and sensing. *Chem. Soc. Rev.* **2013**, *42*, 2824–2860. [[CrossRef](#)]
44. Yavarinasab, A.; Janfaza, S.; Tasnim, N.; Tahmooressi, H.; Dalili, A.; Hoorfar, M. Graphene/poly (methyl methacrylate) electrochemical impedance-transduced chemiresistor for detection of volatile organic compounds in aqueous medium. *Anal. Chim. Acta* **2020**, *1109*, 27–36. [[CrossRef](#)]
45. Qi, F.; Jones, L.O.; Jiang, K.; Jang, S.-H.; Kaminsky, W.; Oh, J.; Zhang, H.; Cai, Z.; Yang, C.; Kohlstedt, K.L. Regiospecific N-alkyl substitution tunes the molecular packing of high-performance non-fullerene acceptors. *Mater. Horiz.* **2022**, *9*, 403–410. [[CrossRef](#)]
46. Abbas, F.; Ali, U.; Ahmad, H.M.R.; Tallat, A.; Shehzad, A.; Zeb, Z.; Hussain, I.; Saeed, A.; Tariq, M. Role of Iodo-Substituted Subphthalocyanine (Subpcs) π -conjugated aromatic N-fused di-Iminoisonidole units on the performance of non-fullerene small organic solar cells. *Comput. Theor. Chem.* **2022**, *1207*, 113508. [[CrossRef](#)]

47. Heredia, D.A.; Durantini, A.M.; Durantini, J.E.; Durantini, E.N. Fullerene C₆₀ derivatives as antimicrobial photodynamic agents. *J. Photochem. Photobiol. C Photochem. Rev.* **2022**, *51*, 100471. [[CrossRef](#)]
48. Baskar, A.V.; Benzigar, M.R.; Talapaneni, S.N.; Singh, G.; Karakoti, A.S.; Yi, J.; Al-Muhtaseb, A.a.H.; Ariga, K.; Ajayan, P.M.; Vinu, A. Self-Assembled Fullerene Nanostructures: Synthesis and Applications. *Adv. Funct. Mater.* **2022**, *32*, 2106924. [[CrossRef](#)]
49. Chen, Z.; Duan, C.; Wang, Z.; Yin, Q.; Huang, F.; Cao, Y. Polythiophene derivatives compatible with both fullerene and non-fullerene acceptors for polymer solar cells. *J. Mater. Chem. C* **2019**, *7*, 314–323.
50. Sun, W.; Lu, G.; Ye, C.; Chen, S.; Hou, Y.; Wang, D.; Wang, L.; Oeser, M. The state of the art: Application of green technology in sustainable pavement. *Adv. Mater. Sci. Eng.* **2018**, *2018*, 9760464. [[CrossRef](#)]
51. Sukumaran, N.P.; Gopi, S. Overview of biopolymers: Resources, demands, sustainability, and life cycle assessment modeling and simulation. In *Biopolymers and Their Industrial Applications*; Elsevier: Amsterdam, The Netherlands, 2021; pp. 1–19.
52. Jebur, Q.M.; Hashim, A.; Habeeb, M.A. Structural, electrical and optical properties for (polyvinyl alcohol–polyethylene oxide–magnesium oxide) nanocomposites for optoelectronics applications. *Trans. Electr. Electron. Mater.* **2019**, *20*, 334–343. [[CrossRef](#)]
53. Oh, S.H.; Vak, D.; Na, S.I.; Lee, T.W.; Kim, D.Y. Water-Soluble Polyfluorenes as an Electron Injecting Layer in PLEDs for Extremely High Quantum Efficiency. *Adv. Mater.* **2008**, *20*, 1624–1629. [[CrossRef](#)]
54. Sasabe, H.; Kido, J. Development of high performance OLEDs for general lighting. *J. Mater. Chem. C* **2013**, *1*, 1699–1707. [[CrossRef](#)]
55. Lan, M.; Zhao, S.; Liu, W.; Lee, C.S.; Zhang, W.; Wang, P. Photosensitizers for photodynamic therapy. *Adv. Healthc. Mater.* **2019**, *8*, 1900132. [[CrossRef](#)]
56. Nalwa, K.S.; Cai, Y.; Thoeming, A.L.; Shinar, J.; Shinar, R.; Chaudhary, S. Polythiophene-fullerene based photodetectors: Tuning of spectral response and application in photoluminescence based (bio) chemical sensors. *Adv. Mater.* **2010**, *22*, 4157–4161. [[CrossRef](#)]
57. Lee, T.-W.; Lim, K.-G.; Kim, D.-H. Approaches toward efficient and stable electron extraction contact in organic photovoltaic cells: Inspiration from organic light-emitting diodes. *Electron. Mater. Lett.* **2010**, *6*, 41–50. [[CrossRef](#)]
58. Hamid, T.; Kielar, M.; Yambem, S.D.; Pandey, A.K. Multifunctional Diode Operation of Tetracene Sensitized Polymer: Fullerene Heterojunctions with Simultaneous Electroluminescence in Visible and NIR Bands. *Adv. Electron. Mater.* **2021**, *7*, 2000824. [[CrossRef](#)]
59. Kang, H.; Kim, G.; Hwang, I.-W.; Kim, Y.; Lee, K.C.; Park, S.H.; Lee, K. High-performance polymer tandem devices combining solar cell and light-emitting diode. *Sol. Energy Mater. Sol. Cells* **2012**, *107*, 148–153. [[CrossRef](#)]
60. Chen, J.-X.; Wang, H.; Zhang, X.; Xiao, Y.-F.; Wang, K.; Zhou, L.; Shi, Y.-Z.; Yu, J.; Lee, C.-S.; Zhang, X.-H. Using Fullerene Fragments as Acceptors to Construct Thermally Activated Delayed Fluorescence Emitters for High-Efficiency Organic Light-Emitting Diodes. *Chem. Eng. J.* **2022**, *435*, 134731. [[CrossRef](#)]
61. Trujillo Herrera, C.; Hong, M.J.; Labram, J.G. Role of the Blend Ratio in Polymer: Fullerene Phototransistors. *ACS Appl. Electron. Mater.* **2020**, *2*, 2257–2264. [[CrossRef](#)]
62. Mariotti, N.; Bonomo, M.; Fagiolari, L.; Barbero, N.; Gerbaldi, C.; Bella, F.; Barolo, C. Recent advances in eco-friendly and cost-effective materials towards sustainable dye-sensitized solar cells. *Green Chem.* **2020**, *22*, 7168–7218. [[CrossRef](#)]
63. Righetto, M.; Meggiolaro, D.; Rizzo, A.; Sorrentino, R.; He, Z.; Meneghesso, G.; Sum, T.C.; Gatti, T.; Lamberti, F. Coupling halide perovskites with different materials: From doping to nanocomposites, beyond photovoltaics. *Prog. Mater. Sci.* **2020**, *110*, 100639. [[CrossRef](#)]
64. Díez-Pascual, A.M.; Rahdar, A. Graphene-Based Polymer Composites for Flexible Electronic Applications. *Micromachines* **2022**, *13*, 1123. [[CrossRef](#)]
65. Savenije, T.J.; Ferguson, A.J.; Kopidakis, N.; Rumbles, G. Revealing the dynamics of charge carriers in polymer: Fullerene blends using photoinduced time-resolved microwave conductivity. *J. Phys. Chem. C* **2013**, *117*, 24085–24103. [[CrossRef](#)]
66. Chung, I.; Song, J.-H.; Im, J.; Androulakis, J.; Malliakas, C.D.; Li, H.; Freeman, A.J.; Kenney, J.T.; Kanatzidis, M.G. CsSnI₃: Semiconductor or metal? High electrical conductivity and strong near-infrared photoluminescence from a single material. High hole mobility and phase-transitions. *J. Am. Chem. Soc.* **2012**, *134*, 8579–8587. [[CrossRef](#)]
67. Coakley, K.M.; Liu, Y.; Goh, C.; McGehee, M.D. Ordered organic–inorganic bulk heterojunction photovoltaic cells. *MRS Bull.* **2005**, *30*, 37–40. [[CrossRef](#)]
68. Kausar, A. Nanodiamond: A multitasking material for cutting edge solar cell application. *Mater. Res. Innov.* **2018**, *22*, 302–314. [[CrossRef](#)]
69. Ito, O.; D'Souza, F. Recent advances in photoinduced electron transfer processes of fullerene-based molecular assemblies and nanocomposites. *Molecules* **2012**, *17*, 5816–5835. [[CrossRef](#)] [[PubMed](#)]
70. Costa, R.D.; Malig, J.; Brenner, W.; Jux, N.; Guldi, D.M. Electron accepting porphycenes on graphene. *Adv. Mater.* **2013**, *25*, 2600–2605. [[CrossRef](#)]
71. Zhang, F.; Ceder, M.; Inganäs, O. Enhancing the photovoltage of polymer solar cells by using a modified cathode. *Adv. Mater.* **2007**, *19*, 1835–1838. [[CrossRef](#)]
72. Kang, Q.; Liao, Q.; Yang, C.; Yang, Y.; Xu, B.; Hou, J. A new PEDOT derivative for efficient organic solar cell with a fill factor of 0.80. *Adv. Energy Mater.* **2022**, *12*, 2103892. [[CrossRef](#)]
73. Chen, L.-M.; Xu, Z.; Hong, Z.; Yang, Y. Interface investigation and engineering—achieving high performance polymer photovoltaic devices. *J. Mater. Chem.* **2010**, *20*, 2575–2598. [[CrossRef](#)]
74. Norrman, K.; Madsen, M.V.; Gevorgyan, S.A.; Krebs, F.C. Degradation patterns in water and oxygen of an inverted polymer solar cell. *J. Am. Chem. Soc.* **2010**, *132*, 16883–16892. [[CrossRef](#)]

75. Kohlstädt, M.; Grein, M.; Reinecke, P.; Kroyer, T.; Zimmermann, B.; Würfel, U. Inverted ITO-and PEDOT: PSS-free polymer solar cells with high power conversion efficiency. *Sol. Energy Mater. Sol. Cells* **2013**, *117*, 98–102. [[CrossRef](#)]
76. Ayzner, A.L.; Tassone, C.J.; Tolbert, S.H.; Schwartz, B.J. Reappraising the need for bulk heterojunctions in polymer– fullerene photovoltaics: The role of carrier transport in all-solution-processed P3HT/PCBM bilayer solar cells. *J. Phys. Chem. C* **2009**, *113*, 20050–20060. [[CrossRef](#)]
77. Campoy-Quiles, M.; Ferenczi, T.; Agostinelli, T.; Etchegoin, P.G.; Kim, Y.; Anthopoulos, T.D.; Stavrinou, P.N.; Bradley, D.D.; Nelson, J. Morphology evolution via self-organization and lateral and vertical diffusion in polymer: Fullerene solar cell blends. *Nat. Mater.* **2008**, *7*, 158–164. [[CrossRef](#)] [[PubMed](#)]
78. Roy, A.; Ghosh, A.; Bhandari, S.; Sundaram, S.; Mallick, T.K. Realization of poly (methyl methacrylate)-encapsulated solution-processed carbon-based solar cells: An emerging candidate for buildings' comfort. *Ind. Eng. Chem. Res.* **2020**, *59*, 11063–11071. [[CrossRef](#)] [[PubMed](#)]
79. Lee, H.K.H.; Telford, A.M.; Röhr, J.A.; Wyatt, M.F.; Rice, B.; Wu, J.; de Castro Maciel, A.; Tuladhar, S.M.; Speller, E.; McGettrick, J. The role of fullerenes in the environmental stability of polymer: Fullerene solar cells. *Energy Environ. Sci.* **2018**, *11*, 417–428. [[CrossRef](#)]
80. Kausar, A. Polymer/fullerene nanocomposite coatings—Front line potential. *Emergent Mater.* **2022**, *5*, 29–40. [[CrossRef](#)]
81. Vohra, V.; Razali, N.T.; Wahi, R.; Ganzer, L.; Virgili, T. A comparative study of low-cost coating processes for green & sustainable organic solar cell active layer manufacturing. *Opt. Mater. X* **2022**, *13*, 100127.
82. Amb, C.M.; Craig, M.R.; Koldemir, U.; Subbiah, J.; Choudhury, K.R.; Gevorgyan, S.A.; Jørgensen, M.; Krebs, F.C.; So, F.; Reynolds, J.R. Aesthetically pleasing conjugated polymer: Fullerene blends for blue-green solar cells via roll-to-roll processing. *ACS Appl. Mater. Interfaces* **2012**, *4*, 1847–1853. [[CrossRef](#)]
83. Khlyabich, P.P.; Burkhart, B.; Rudenko, A.E.; Thompson, B.C. Optimization and simplification of polymer–fullerene solar cells through polymer and active layer design. *Polymer* **2013**, *54*, 5267–5298. [[CrossRef](#)]
84. Pellis, A.; Byrne, F.P.; Sherwood, J.; Vastano, M.; Comerford, J.W.; Farmer, T.J. Safer bio-based solvents to replace toluene and tetrahydrofuran for the biocatalyzed synthesis of polyesters. *Green Chem.* **2019**, *21*, 1686–1694. [[CrossRef](#)]
85. Lee, S.; Jeong, D.; Kim, C.; Lee, C.; Kang, H.; Woo, H.Y.; Kim, B.J. Eco-friendly polymer solar cells: Advances in green-solvent processing and material design. *ACS Nano* **2020**, *14*, 14493–14527. [[CrossRef](#)]
86. Kim, J.Y.; Lee, J.-W.; Jung, H.S.; Shin, H.; Park, N.-G. High-efficiency perovskite solar cells. *Chem. Rev.* **2020**, *120*, 7867–7918. [[CrossRef](#)]
87. Li, B.; Wu, X.; Zhang, H.; Zhang, S.; Li, Z.; Gao, D.; Zhang, C.; Chen, M.; Xiao, S.; Jen, A.K.Y. Efficient and Stable Tin Perovskite Solar Cells by Pyridine-Functionalized Fullerene with Reduced Interfacial Energy Loss. *Adv. Funct. Mater.* **2022**, *32*, 2205870. [[CrossRef](#)]
88. Castro, E.; Murillo, J.; Fernandez-Delgado, O.; Echegoyen, L. Progress in fullerene-based hybrid perovskite solar cells. *J. Mater. Chem. C* **2018**, *6*, 2635–2651. [[CrossRef](#)]
89. Roseela, J.A.; Godhvari, T.; Narayanan, R.; Madhuri, P. Design and deployment of IoT based underwater wireless communication system using electronic sensors and materials. *Mater. Today Proc.* **2020**, *45*, 6229–6233. [[CrossRef](#)]
90. Wu, M.; Chen, J.; Ma, Y.; Yan, B.; Pan, M.; Peng, Q.; Wang, W.; Han, L.; Liu, J.; Zeng, H. Ultra elastic, stretchable, self-healing conductive hydrogels with tunable optical properties for highly sensitive soft electronic sensors. *J. Mater. Chem. A* **2020**, *8*, 24718–24733. [[CrossRef](#)]
91. Eom, T.H.; Kim, T.; Jang, H.W. Hydrogen Sensing of Graphene-based Chemoresistive Gas Sensor Enabled by Surface Decoration. *J. Sens. Sci. Technol.* **2020**, *29*, 382–387. [[CrossRef](#)]
92. Mirzaei, A.; Kim, J.-H.; Kim, H.W.; Kim, S.S. Resistive-based gas sensors for detection of benzene, toluene and xylene (BTX) gases: A review. *J. Mater. Chem. C* **2018**, *6*, 4342–4370. [[CrossRef](#)]
93. Shi, G.; Meng, Q.; Zhao, Z.; Kuan, H.-C.; Michelmore, A.; Ma, J. Facile fabrication of graphene membranes with readily tunable structures. *ACS Appl. Mater. Interfaces* **2015**, *7*, 13745–13757. [[CrossRef](#)]
94. Cahen, D.; Naaman, R.; Vager, Z. The cooperative molecular field effect. *Adv. Funct. Mater.* **2005**, *15*, 1571–1578. [[CrossRef](#)]
95. Della Pelle, F.; Angelini, C.; Sergi, M.; Del Carlo, M.; Pepe, A.; Compagnone, D. Nano carbon black-based screen printed sensor for carbofuran, isoprocarb, carbaryl and fenobucarb detection: Application to grain samples. *Talanta* **2018**, *186*, 389–396. [[CrossRef](#)]
96. Xiao, Z.; Kong, L.B.; Ruan, S.; Li, X.; Yu, S.; Li, X.; Jiang, Y.; Yao, Z.; Ye, S.; Wang, C. Recent development in nanocarbon materials for gas sensor applications. *Sens. Actuators B Chem.* **2018**, *274*, 235–267. [[CrossRef](#)]
97. Colak, O.; Arslan, H.; Zengin, H.; Zengin, G. Amperometric detection of glucose by polyaniline-activated carbon composite carbon paste electrode. *Int. J. Electrochem. Sci.* **2012**, *7*, 6988–6997.
98. Pilan, L.; Raicopol, M. Highly selective and stable glucose biosensors based on polyaniline/carbon nanotubes composites. *UPB Sci. Bull. Ser. B* **2014**, *76*, 155–166.
99. Ruecha, N.; Rodthongkum, N.; Cate, D.M.; Volckens, J.; Chailapakul, O.; Henry, C.S. Sensitive electrochemical sensor using a graphene–polyaniline nanocomposite for simultaneous detection of Zn (II), Cd (II), and Pb (II). *Anal. Chim. Acta* **2015**, *874*, 40–48. [[CrossRef](#)]
100. Nasresfahani, S.; Sheikhi, M.; Tohidi, M.; Zarifkar, A. Methane gas sensing properties of Pd-doped SnO₂/reduced graphene oxide synthesized by a facile hydrothermal route. *Mater. Res. Bull.* **2017**, *89*, 161–169. [[CrossRef](#)]
101. Kooti, M.; Keshtkar, S.; Askarieh, M.; Rashidi, A. Progress toward a novel methane gas sensor based on SnO₂ nanorods-nanoporous graphene hybrid. *Sens. Actuators B Chem.* **2019**, *281*, 96–106. [[CrossRef](#)]

102. Ruecha, N.; Rangkupan, R.; Rodthongkum, N.; Chailapakul, O. Novel paper-based cholesterol biosensor using graphene/polyvinylpyrrolidone/polyaniline nanocomposite. *Biosens. Bioelectron.* **2014**, *52*, 13–19. [[CrossRef](#)]
103. Niu, P.; Fernández-Sánchez, C.; Gich, M.; Navarro-Hernández, C.; Fanjul-Bolado, P.; Roig, A. Screen-printed electrodes made of a bismuth nanoparticle porous carbon nanocomposite applied to the determination of heavy metal ions. *Microchim. Acta* **2016**, *183*, 617–623. [[CrossRef](#)]
104. Cinti, S.; Santella, F.; Moscone, D.; Arduini, F. Hg²⁺ detection using a disposable and miniaturized screen-printed electrode modified with nanocomposite carbon black and gold nanoparticles. *Environ. Sci. Pollut. Res.* **2016**, *23*, 8192–8199. [[CrossRef](#)]
105. Clifford, J.P.; Konstantatos, G.; Johnston, K.W.; Hoogland, S.; Levina, L.; Sargent, E.H. Fast, sensitive and spectrally tuneable colloidal-quantum-dot photodetectors. *Nat. Nanotechnol.* **2009**, *4*, 40–44. [[CrossRef](#)]
106. Ishimatsu, R.; Naruse, A.; Liu, R.; Nakano, K.; Yahiro, M.; Adachi, C.; Imato, T. An organic thin film photodiode as a portable photodetector for the detection of alkylphenol polyethoxylates by a flow fluorescence-immunoassay on magnetic microbeads in a microchannel. *Talanta* **2013**, *117*, 139–145. [[CrossRef](#)]
107. Kraker, E.; Haase, A.; Lamprecht, B.; Jakopic, G.; Konrad, C.; Köstler, S. Integrated organic electronic based optochemical sensors using polarization filters. *Appl. Phys. Lett.* **2008**, *92*, 18. [[CrossRef](#)]
108. Amao, Y. Probes and polymers for optical sensing of oxygen. *Microchim. Acta* **2003**, *143*, 1–12. [[CrossRef](#)]
109. Augusto, V.; Baleizao, C.; Berberan-Santos, M.N.; Farinha, J.P.S. Oxygen-proof fluorescence temperature sensing with pristine C₇₀ encapsulated in polymer nanoparticles. *J. Mater. Chem.* **2010**, *20*, 1192–1197. [[CrossRef](#)]
110. Yakuphanoglu, F.; Kandaz, M.; Senkal, B.F. Inorganic–organic photodiodes based on polyaniline doped boric acid and polyaniline doped boric acid: Nickel (II) phthalocyanine composite. *Sens. Actuators A Phys.* **2009**, *153*, 191–196. [[CrossRef](#)]
111. Amao, Y.; Okura, I. Fullerene C₆₀ immobilized in polymethylmethacrylate film as an optical temperature sensing material. *Analisis* **2000**, *28*, 847–849. [[CrossRef](#)]
112. Rather, J.A.; De Wael, K. Fullerene-C₆₀ sensor for ultra-high sensitive detection of bisphenol-A and its treatment by green technology. *Sens. Actuators B Chem.* **2013**, *176*, 110–117. [[CrossRef](#)]
113. Zhang, M.; Li, J. Preparation of porphyrin derivatives and C₆₀ supramolecular assemblies as a sensor for detection of dopamine. *Dye. Pigment.* **2020**, *173*, 107966. [[CrossRef](#)]
114. Chen, J.; Jia, C.; Wan, Z. Novel hybrid nanocomposite based on poly (3, 4-ethylenedioxythiophene)/multiwalled carbon nanotubes/graphene as electrode material for supercapacitor. *Synth. Met.* **2014**, *189*, 69–76. [[CrossRef](#)]
115. Lawal, A.T.; Wallace, G.G. Vapour phase polymerisation of conducting and non-conducting polymers: A review. *Talanta* **2014**, *119*, 133–143. [[CrossRef](#)]
116. Moussa, M.; El-Kady, M.F.; Zhao, Z.; Majewski, P.; Ma, J. Recent progress and performance evaluation for polyaniline/graphene nanocomposites as supercapacitor electrodes. *Nanotechnology* **2016**, *27*, 442001. [[CrossRef](#)]